J. Synchrotron Rad. (1999). **6**, 258–260

Pre-edge structure analysis of Ti *K*-edge polarized X-ray absorption spectra in TiO$_2$ by full-potential XANES calculations

Delphine Cabaret,[a]* Yves Joly,[b] Hubert Renevier[b] and Calogero R. Natoli[c]

[a]Laboratoire de Minéralogie-Cristallographie, Universités Paris VI et VII, Tour 16, case courrier 115, 4 place Jussieu, 75252 Paris cedex 05 France, [b]Laboratoire de Cristallographie, CNRS, associé à l'Université Joseph Fourier, B.P. 166, 38042 Grenoble Cedex France , and [c]Laboratori Nazionali di Frascati, INFN, Casella Postale 13, 00044 Frascati Italy. E-mail: cabaret@lmcp.jussieu.fr

The pre-edge region of Ti K-edge polarized XANES spectra in TiO$_2$-rutile is investigated by full-potential calculations based on the finite-difference method. Both dipolar and quadrupolar transitions are considered. The use of "non muffin-tin" potential allows a clear interpretation of the pre-edge features. The results are consistent with Full-potential LAPW band structure calculations, and are also compared with multiple-scattering calculations.

keywords : XANES calculations, finite-difference method, pre-edge structure, TiO$_2$-rutile

1. Introduction

The understanding of the chemical and electronic properties of titanium oxides is of great interest in catalysis, geological sciences, and high-T$_c$ superconductivity (Kung, 1989; Farges *et al.*, 1997, Durmeyer *et al.*, 1990). Core level spectroscopies are known to be a good tool for such purposes and have been exploited for various titanium oxides (Farges *et al.*; Wu *et al.*, 1997 and references therein). This paper deals with the rutile phase of TiO$_2$ which became an excellent case for testing new developments in band-structure methods (Hamann *et al.*, 1997). Although its electronic structure is now assumed to be well-known (Hardman *et al.*, 1994; Sorantin & Schwarz, 1992; Glassford & Chelikowsky,1992; Khan *et al.*, 1991; Poumellec *et al.*, 1991*b*), there is still a doubt about the interpretation of its x-ray absorption pre-edge structure at the Ti K-edge, which is composed of three well defined features (usually labelled A$_1$, A$_2$ and A$_3$). Indeed the pre-edge region is the subject of a large debate not closed yet: in section V-E, Farges *et al.* (1997) recall the recent studies of the pre-edge structure. All the cited interpretations are made from the isotropic spectrum, for which the agreement between theory and experiment is quite satisfying (Ruiz-Lòpez & Muñoz-Páez, 1991; Poumellec *et al.*, 1991*b*; Wu *et al.*, 1997). But when polarized spectra are investigated, some discrepancies between the calculated and experimental curves are encountered especially in the pre-edge region; the angular dependence is not reproduced (Farges, 1998). In calculations mentioned above, the optical potential seen by the photoelectron is constructed in the "muffin-tin" approximation. In this latter, the potential is spherically symmetric in non-overlapping spheres defined around each atom, and constant in the interatomic region. As written by Sorantin & Schwarz (1992) this approximation is "only tolerable in close-packed structures, but certainly not for rutile-type compounds". This is particularly true in the pre-edge region where the excited photoelectron becomes rather sensitive to the spatial and electronic details of the potential.

In order to correctly reproduce the pre-edge features of the Ti K-edge XANES of TiO$_2$, we used the "non muffin-tin" approach presented by Joly (1997) at the XAFS-IX Conference: it is a new scheme of XANES calculation based on the finite-difference method (FDM). This latter is a general way to solve differential equations as the Schrödinger equation. It does not require any approximation on the shape of the potential, so the usual "muffin-tin" approximation is avoided as well as the problem of near field corrections. Starting from a convenient electron density, the full-potential (FP) can then be constructed solving the Poisson equation and using an Hedin-Lundqvist treatment of the exchange and correlation potential. For comparison two different approaches were used to calculate the electron density. The first uses the self-consistent Full-potential Linearized Augmented Plane Wave (FLAPW) method developed by Blaha *et al.* (1990) in the `Wien97` package. The second uses a fit procedure of the experimental XANES spectra. In that case a simple superimposition of the atomic electronic density is performed, the optimized parameters being the electronic ocupation number on each valence orbitals. As will be discussed in the next section both approaches are in agreement, but the second one has the advantage to be able to describe the screening charge on the photoabsorber and to be usable when the material is not periodic. As the analysis of the charge exchange between atoms, this point goes beyond the scope of this paper and is not discussed more here. Both dipolar and quadrupolar transitions were considered in the photoabsorption cross section. The cluster size convergence was reached for 93 atoms (radius of 6.9 Å) and the calculated spectra were convoluted by a Lorentzian function.

The calculated spectra are compared with the angular-dependent experiments of Poumellec *et al.* (1991*a*). The chosen setups for the directions of the electric field and of the propagation vector are: (1): $(\varepsilon, \mathbf{k}) = ([001], [110])$ and (2): $(\varepsilon, \mathbf{k}) = ([1\bar{1}0], [110])$. According to the crystallographic structure of TiO$_2$ rutile (Sorantin & Schwarz, 1992), the symmetry type of the orbitals reached in the final state is: (1) p_z for the dipolar transition and d_{xz} and d_{yz} for the quadrupolar, (2) p_x and p_y for the dipolar and only d_{xy} for the quadrupolar.

2. Results and discussion

The results of the FP-XANES calculations are presented in Fig. 1(a) for the two setups (1) and (2). The calculated curves are overlayed to experiments. For both polarizations an excellent agreement is obtained. All the features, even in the pre-edge region, are well reproduced. In particular the splitting of the main peak C for $\varepsilon \parallel z$ into two peaks C$_1$ and C$_2$ when $\varepsilon \perp z$ is also reproduced. The potential used here results from the superimposition of atomic charge densities. A 1s electron was promoted to a 3d orbital for the central photoabsorbing Ti atom to modelize the excited state. The spectra calculated with the ground state self-consistent potential extracted from the FLAPW framework leads to the same result in the dipolar approximation. Indeed the dipolar spectrum is not affected by the core-hole effects: it reflects density of states related to medium range order in the compound. For comparison band structure calculation were performed again within the framework of the FLAPW method, obtaining agreement with similar calculations by Sorantin & Schwarz (1992). The p_z and (p_x, p_y) projected density of states (DOS) on Ti atom are shown in Fig. 1(b). Above 12 eV, the Ti-p_z DOS exhibits two main peaks associated with peaks C

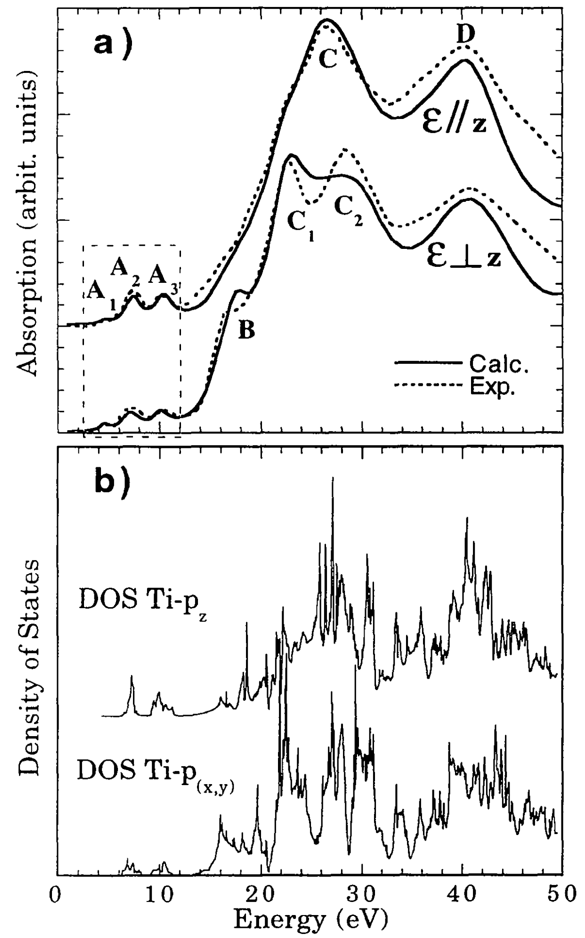

Figure 1

a) Comparison between FP-XANES calculations (full line) and experimental spectra (dotted line) at the Ti K-edge in TiO_2 for two polarizations of the incident beam : $(\varepsilon,\mathbf{k}) = ([001],[110])$ (top), $(\varepsilon,\mathbf{k}) = ([1\bar{1}0],[110])$ (bottom). b) Ti-p_z (top) and Ti-(p_x,p_y) (bottom) density of states calculated by the FLAPW method.

and D of the experimental spectrum. The Ti-$p_{(x,y)}$ DOS is separate into four main peaks located at energy position corresponding to B, C_1, C_2 and D experimental features. In the pre-edge region, the DOS exhibits two peaks that come from the hybridization between the $4p$ orbitals and the $3d$ orbitals split into their t_{2g}-*like* and e_g-*like* components by the crystal field, and that are related to the A_2 and A_3 experimental peaks.

A view of the pre-edge region of FP-XANES calculations is displayed on Fig. 2. One observes that A_2 and A_3 are higher when $\varepsilon \parallel z$ than when $\varepsilon \perp z$. On the contrary A_1 is lower in the first polarization. This is well reproduced by the calculation as well as the shape of A_2 whose width is larger for $\varepsilon \perp z$. The dipolar (d) and the quadrupolar (q) components are also plotted. As experimentally shown by Brouder *et al.* (1990), we found that the quadrupolar contribution is significant. Moreover this latter is extremely sensitive to the core-hole effects, contrary to the dipole component which is insensitive to the screening charge, as shown before. A_1 is only quadrupolar t_{2g}, A_2 is dipolar in nature but includes also a little e_g quadrupolar component; A_3 is a pure dipolar component. A_2 and A_3 are related to medium range order through the hybridization of the central Ti-$4p$ orbital with the second shell Ti-$3d$ orbitals.

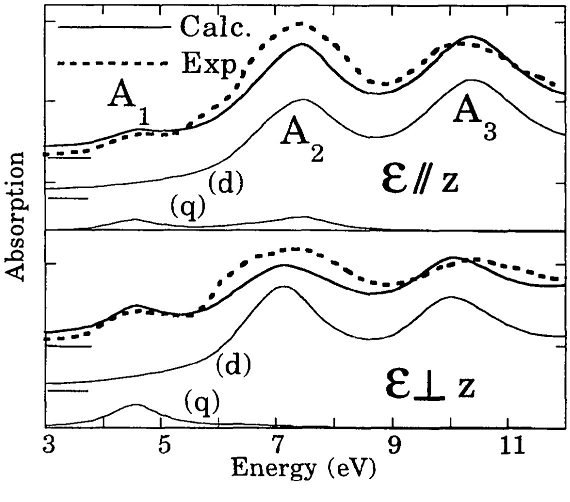

Figure 2

View of the pre-edge region of Fig 1(a). Quadrupolar (q) and dipolar (d) components are also plotted under the experimental (dotted) and calculated (full) overlayed curves.

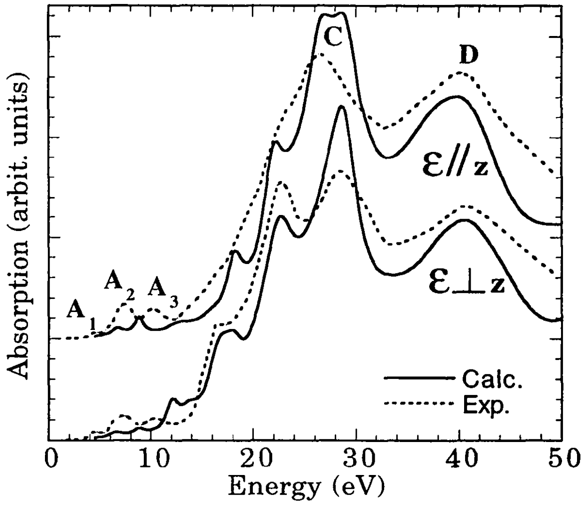

Figure 3

Comparison between "muffin-tin" multiple-scattering calculations (full line) and experimental spectra (dotted line) at the Ti K-edge in TiO_2 for both polarizations.

Concerning the assignment of A_2 and A_3 our results are consistent with those of Poumellec *et al.* (1991*b*), who calculated the Ti-K pre-edge region from the p-projected DOS of titanium and terms dependent only of the potential, both determined within the self-consistent LMTO-ASA framework. Their method is quite successful in the pre-edge region but fails to reproduce the spectrum above A_3 peak. Our results are in total agreement with Uozomi *et al.* (1992), who notably attribute A_1 to a quadrupolar transition of t_{2g} symmetry. But they differ from those of Wu *et al.* (1997) and of Brydson *al.* (1991) who, relying on "muffin-tin" calculations, attribute the A$_1$ feature to a dipolar transition. We have also performed "muffin-tin" calculations in the dipolar approximation, as shown in Fig. 3. Experimental spectra are overlayed to multiple-scattering calculations performed with the Continuum Code developed by Natoli *et al.* (1980). The cluster potential is the same as the one described by Wu *et al.* (1997): in particular the X-α exchange and correlation potential was added to the Coulomb part and the convergence was obtained for a 93 atom cluster. The convergence of the basis functions for the final state was reached for $\ell_{max} = 4$ where ℓ_{max} is the maximum orbital angular momentum. The calculated spectra were convoluted by the same Lorentzian than the FP-XANES calculations. In Fig. 3, the agreement between calculations and experiments is quite good except in the pre-edge region. In the near-edge region, all the calculated features are located at the good energy positions but their relative intensities are not reproduced. In the pre-edge region, the agreement is so poor that valuable information can hardly be extracted. We have also tested a Hedin-Lundqvist exchange and correlation potential as within the FP framework, but it does not improve the agreement. As emphasized by Wu *et al.* (1997), the X-α potential is not a limitation at low energies ($<$ 30 eV above the threshold) since it is very close to the real part of the Hedin-Lundqvist one if the α constant is appropriately chosen. Now let us compare our angular-dependent spectra of Fig. 3 with the results related to the isotropic spectrum present in the literature. Our results are consistent with the Feff calculations performed by Farges *et al.* (1997). Obviously they are also similar to those of Wu *et al.* (1997). In their paper the direct comparison with experiment is made difficult since the spectra are not displayed in the same figure. In Brydson *et al.* (1991) most features are reproduced but the agreement in relative intensities remains very bad. It is thus quite hasardous to derive some conclusion from the calculation.

Finally, although multiple-scattering theory has proved to be a powerful technique to extract information from XANES spectra, the results obtained at the Ti K-edge are not satisfactory as compared with the FP-XANES calculations. Therefore, on the basis of the present findings, the results of Wu *et al.* (1997) and Brydson *et al.* (1991) concerning the assignment of A$_1$ are clearly an artefact of the "muffin-tin" approximation.

Summarizing, we hope to have given a convincing interpretation of the pre-edge structure of the Ti K-edge XANES spectrum. This was achieved by performing "non muffin-tin" calculations, based on the finite difference method. An excellent agreement with experiment was obtained. FLAPW band structure calculations were also performed and are consistent with the results. Furthermore, this study suggests that XANES calculated using the FDM method to solve the Schrödinger equation for the photoelectron moving in an effective optical potential of the local-density type, can become a quite reliable tool for obtaining parameters related to the electronic structure of the system under study. This last point will be developed in a forthcoming publication.

Computing time was partly supplied by the "Institut du Développement et des Ressources Informatiques Scientifiques". We would like to thank François Farges and Christian Brouder for fruitful discussions.

References

Blaha, P., Schwarz, K., Sorantin, P. & Trickey, S. (1990). *Comp. Phys. Commun.* **59**, 399–415.

Brouder, C., Kappler, J.-P. & Beaurepaire, E. (1990). In *2nd European Conference on Progress in X-ray Synchrotron Radiation Research*, edited by A. Balerna, E. Bernieri & S. Mobilio, vol. 25, pp. 19–21. Bologna: Editrice Compositori.

Brydson, R., Sauer, H., Engel, W., Thomas, J., Zeitler, E., Kosugi, N. & Kuroda, H. (1989). *J. Phys.: Condens. Matter*, **1**, 797–812.

Durmeyer, O., Kappler, J.-P., Beaurepaire, E., Heintz, J.-M. & Drillon, M. (1990). *J. Phys.: Condens. Matter*, **2**, 6127–6136.

Farges, F., (1998). Personal communication.

Farges, F., Brown, Jr., G. & Rehr, J. (1997). *Phys. Rev. B*, **56**, 1809–1819.

Glassford, K. & Chelikowsky, J. (1992). *Phys. Rev. B*, **46**, 1284–1298.

Hamann, D. (1997). *Phys. Rev. B*, **56**, 14979–14984.

Hardman, P., Raikar, G., Muryn, C., van der Laan, G., Wincott, P., Thornton, G., Bullet, D. & Dale, P. (1994). *Phys. Rev. B*, **49**, 7170–7177.

Joly, Y. (1997). In *Proceedings of the XAFS IX Conference, J. Phys. IV France, Colloque C2*, vol. 7, pp. C2-111-115.

Khan, M. A., Kotani, A. & Parlebas, J. C. (1991). *J. Phys.: Condens. Matter*, **3**, 1763–1772.

Kung, H. (1989). In *Transition Metal Oxides*, edited by B. Delmon & J. Yates, vol. 45, chap. 10 and 14. Amsterdam: Elsevier.

Natoli, C. R., Misemer, D. K. & Doniach, S. (1980). *Phys. Rev. A*, **22**, 1104–1108.

Poumellec, B., Cortes, R., Tourillon, G. & Berthon, J. (1991*a*). *Phys. Stat. Sol. (b)*, **164**, 319–326.

Poumellec, B., Durham, P. J. & Guo, G. Y. (1991*b*). *J. Phys.: Condens. Matter*, **3**, 8195–8204.

Ruiz-Lòpez, M. F. & noz Páez, A. M. (1991). *J. Phys.: Condens. Matter*, **3**, 8981–8990.

Sorantin, P. I. & Schwartz, K. (1992). *Inorg. Chem. Phys.* **31**, 567–576.

Uozumi, T., Okada, K., Kotani, A., Durmeyer, O., Kapler, J.-P., Beaurepaire, E. & Parlebas, J. C. (1992). *Europhys. Lett.* **18**, 85–90.

Wu, Z. Y., Ouvrard, G., Gressier, P. & Natoli, C. R. (1997). *Phys. Rev. B*, **55**, 10382–10391.

(Received 10 August 1998; accepted 14 January 1999)